Soft Matter

Accepted Manuscript

ROYAL SOCIETY
OF **CHEMISTRY**

www.rsc.org/softmatter

T1 Process and Dynamics in Glass-Forming Hard-sphere Liquids

Yuxing Zhou and Scott T. Milner*

Received Xth XXXXXXXXXX 20XX, Accepted Xth XXXXXXXXX 20XX
First published on the web Xth XXXXXXXXXX 200X
DOI: 10.1039/b000000x

To study the relationship between dynamics and structure in a glass-forming liquid, we introduce a purely geometric criterion for locally mobile particles in a dense hard-sphere fluid: namely, “T1-active” particles, which can gain or lose at least one Voronoi neighbor by moving within their free volume with other particles fixed. We obtain geometrical and dynamical properties for monodisperse hard-sphere fluids with $0.40 < \phi < 0.64$ using a “crystal-avoiding” MD simulation that effectively suppresses crystallization without altering the dynamics. We find that the fraction of T1-active particles vanishes at random close packing, while the percolation threshold of T1-inactive particles is essentially identical to the commonly identified hard-sphere glass transition, $\phi_g \approx 0.585$.

1 Introduction

The dramatic slowing down and heterogeneity of dynamics in glass-forming liquids is related to growth of regions of particles that require collective rearrangements to relax. Despite substantial efforts, the structural origin of glass transition remains unclear. Widmer-Cooper et al., demonstrated that local Debye-Waller factor of a particle (corresponding to the short time dynamics or ”rattling motion”) is correlated with its dynamical propensity (characterizing long time dynamics or “cage-breaking” process)[1]. Both quantities were obtained from an isoconfigurational ensemble average, in which multiple simulations are performed with the same starting configuration and different realizations of thermal initial velocities. Hence both the Debye-Waller factor and the propensity only depend on the initial geometry. Similarly, recent numerical and experimental results suggest a strong correlation between irreversible structural reorganization and quasi-localized soft modes, which again reflect the local structure[2,3]. However, finding a local measure of the initial configuration that is causally connected to the dynamics has proven to be elusive[4].

In this paper, we propose a new, purely geometrical criterion that relates directly to the hard-sphere glass transition. By analogy to rearrangement processes in foams, we define “T1-active” particles as those that can either gain or lose a Voronoi neighbor by moving within their own free volumes, with other particles held fixed. When T1-inactive particles percolate, we may expect the system to become non-ergodic or glassy. In fact, we find that the percolation threshold of T1-inactive particles coincides with the monodisperse hard-sphere glass transition, commonly reported at $\phi_g \approx 0.585$[5,6].

2 Method

Hard-sphere fluids have been intensively studied since they serve as the simplest model that exhibits a glass transition, and are well approximated by real colloidal suspensions. Geometric properties such as free volume and cavities can be defined rigorously and computed conveniently for hard-sphere systems[7]. However, monodisperse hard-sphere fluids crystallize readily at volume fractions $\phi > \phi_f \approx 0.494$. To study the metastable fluid phase above ϕ_g, a small amount of polydispersity δ (defined as the fractional standard deviation of particle diameter) is typically introduced to suppress crystallization. Recently, the extent to which polydispersity alters the dynamics near the glass transition has been debated[8–10]. Also, algorithms for computing free volume and related properties are most conveniently implemented for monodisperse hard-spheres (though extension to polydisperse spheres is possible)[7]. For these reasons, it would be attractive to find a way to carry out molecular dynamics (MD) simulations of monodisperse hard-sphere fluids in which crystallization was somehow suppressed.

We have developed a crystal-avoiding (CA) MD simulation method based on hybrid Monte Carlo (MC), inspired by previous works[12–15]. Each MC move is generated from a short event-driven MD trajectory and accepted with a probability $p = \min\{\exp(-\gamma N \Delta \hat{q}_6), 1\}$, where N is the number of particles and $\hat{q}_6$ is the local bond order parameter averaged over next-nearest neighbors[16] (or any other sensitive bond-order parameter that measures the crystallinity of the system). If the MC move is rejected, all particle velocities are reassigned from a Maxwell-Boltzmann distribution before the next trial

---

Department of Chemical Engineering, Pennsylvania State University, University Park, State College, PA, 16803, USA. E-mail: stm9@psu.edu; Fax: +1-814-865-7846; Tel: +1- 814-863-9355

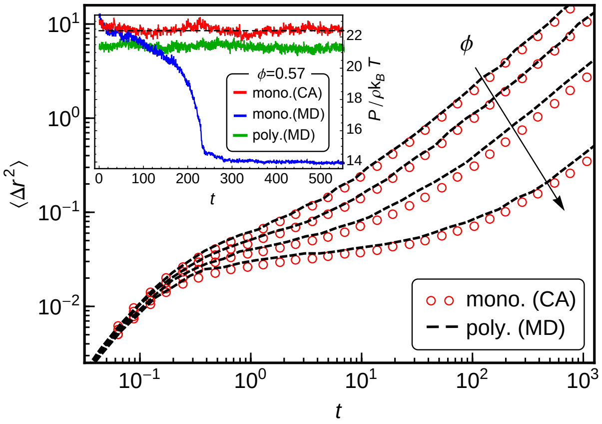

Fig. 1 Mean-squared displacements for monodisperse hard spheres using crystal-avoiding method (CA) and polydisperse systems with conventional MD (MD) at $\phi = 0.55$, 0.56, 0.57 and 0.58. Inset: pressure versus time at $\phi = 0.57$ with different methods. Dotted line indicates corresponding pressure reported in Ref.[11].

move. We emphasize that the simulation time only advances when a trial is accepted; in this way, the particle dynamics can be reasonably reproduced despite the low acceptance rate. In short, the method essentially samples among those trajectories in phase space for which crystallization did not occur. If the duration of the trial trajectories and hence the time between velocity randomizations is larger than velocity autocorrelation time, the resulting dynamics should well represent the metastable fluid. If nucleation is rapid, this may lead to a low acceptance rate of trial moves. In practice, we choose the bias γ and trial trajectory length l_{MD} for reasonably high acceptance rates and fidelity to dynamics of polydisperse systems (see Table 1).

Fig.2 illustrates the dependence of the particle self-diffusion coefficient D on the crystal bias parameter γ and trial trajectory length l_{MD}, for a dense system with $\phi = 0.56$. The self-diffusion coefficient is clearly insensitive to the value of γ (over this range, crystallinity is effectively suppressed). D depends weakly on l_{MD}, until l_{MD} becomes longer than the particle velocity autocorrelation time. For the largest values of ϕ we study $\phi \geq 0.57$, to maintain a reasonable acceptance rate, we take smaller l_{MD} values (10–20, see Table 1). This leads to slightly smaller values of D (by a factor of $10^{0.15} \approx 1.4$), which is a small effect compared to the strong dependence of D on ϕ.

We test the CA method by comparing to monodisperse and mildly polydisperse systems (Gaussian distributed diameters with $\delta = 0.08$) at $\phi = 0.57 > \phi_{\mathrm{f}}$ simulated with conventional MD. The inset to Fig. 1 shows that a monodisperse system under MD will crystallize spontaneously as indicated by an abrupt drop in pressure. The same monodisperse system simulated with the CA method maintains a constant pressure, indicating that crystallization is suppressed. Likewise, a polydisperse system under MD does not crystallize — but does display a lower constant pressure, as noted previously[5]. On the other hand, the mean-squared displacement (MSD) of systems simulated with the CA method are consistent with those of polydisperse systems under MD. Previous work suggests that MSD is insensitive to the amount of mild polydispersity[6] as long as the system is below glass transition, so we conclude the dynamics of metastable monodisperse fluids are well represented by our CA method.

In contrast, for systems at or slightly above the glass transition, we observe a dramatic difference in the dynamics of monodisperse and slightly polydisperse systems. Fig. 3 compares the dependence of the apparent particle diffusion coefficient on aging time t_{e} (time elapsed after the initial Lubachevsky-Stillinger configurations are generated, before the diffusion coefficient is measured). For $\phi = 0.58$, both monodisperse (filled symbols) and slightly polydisperse systems (open symbols) show no dependence of D on aging. For $\phi = 0.59$ — slightly above the commonly reported colloidal glass transition of $\phi_{\mathrm{c}} = 0.585$[5,6] — the monodisperse system shows a strong aging dependence of D, which continues to decrease with t_{e} as far as we can observe. (The inset shows two representative plots of Δr^2 versus t for the monodisperse system for different aging times; values of D are extracted from the slopes of these plots.) The polydisperse system displays some aging dependence, but ultimately seems to settle to a finite value of D. This contrast between the sudden onset of strong aging in the monodisperse system and the more modest aging behavior of the polydisperse system suggests that the polydisperse glass transition is smeared or delayed due to small mobile particles, consistent with recent findings by Zaccarelli et al.[10].

For our simulations of metastable monodisperse hard-sphere fluids, we use the Lubachevsky-Stillinger algorithm[17]

Table 1 Parameters for crystal-avoiding MD simulation. MD trial length l_{MD} is in unit of collisions per particle. The smaller l_{MD} used for high ϕ is a compromise between reproducing dynamics and high acceptance rate (see main text).

ϕ	γ	l_{MD}
< 0.50	0	-
0.50 – 0.53	0.25	40
0.54	0.50	40
0.55	0.50	40
0.56	1.00	40
0.57	1.20	20
0.58	1.20	10
≥ 0.59	1.50	10

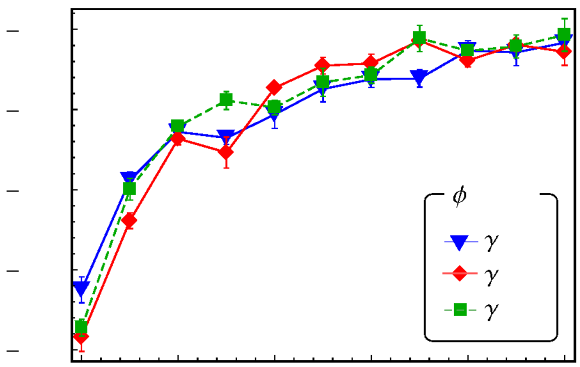

Fig. 2 Dependence on γ and l_{MD} of diffusion coefficients D at $\phi = 0.56$. The resulting dynamics is insensitive to γ and depends weakly on l_{MD} (see main text). For reference, $\log_{10} D \approx -4.0$ for $\gamma = 0$ (crystal) as shown in Fig. 5a.

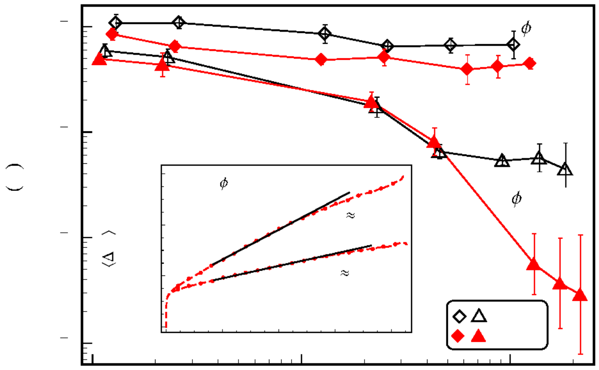

Fig. 3 Dependence on equilibration time τ_e of diffusion coefficients $D(t_e)$ at $\phi = 0.58$ and $\phi = 0.59$ with filled and empty symbols representing monodisperse and polydisperse systems, respectively. Inset: examples of obtaining $D(t_e)$ from the slope of MSD in monodisperse systems at $\phi = 0.59$ for different t_e.

to prepare initial fluid configurations of $N = 2000$ hard spheres with $\phi = 0.40$ to 0.61. Then, we use the CA method to equilibrate the systems until no obvious aging process is observed for the quantity of interest before collecting data. (For $\phi \geq 0.59$, data are collected after the longest equilibration time we can perform in spite of the aging.) The fraction of "crystalline particles" is controlled to be less than 3%. (A particle i is deemed crystalline if it has $N_c \geq 6$ neighbors with local bond order parameter $d_6(i, j) > 0.7$, see Ref.[18].) Polydisperse systems are also prepared using Lubachevsky-Stillinger algorithm with diameters normally distributed. Standard hard-sphere units are used: sphere diameter σ, sphere mass m, collision time $\tau = \sigma\sqrt{m/(k_{\mathrm{B}}T)}$.

3 Results

In this work, we are concerned with local geometries that permit particles to rearrange. Such rearrangements or "cage-breaking" events are often identified by comparing particle displacements to a threshold. As we shall show, such events can equally well be identified by counting the number of changed Voronoi neighbors. In this language, the "supercooling" (densification) of a hard-sphere fluid can be described as follows. For $\phi < \phi_g$, particles change neighbors frequently and irreversibly, and the system is ergodic. Above ϕ_g, more and more neighbors are fixed during a given time, and ergodicity is broken. At $\phi = \phi_J$, the system is completely jammed, and no particle can change any neighbors.

To establish the connection between mobility and neighbor rearrangements, we compare the dynamic propensity $\langle \Delta r_i^2 \rangle_{ic}$, calculated following Ref.[19], and the total number of new Voronoi neighbors, defined as $|\cup_j \mathbf{V}_{ij}|$, where $\mathbf{V}_{ij}$ is the set of new neighbors that particle i gained in the jth isoconfigurational run, starting from the same initial configuration. Here $|\cup_j \mathbf{V}_{ij}|$ is a short-time measure of rearrangements, in that we take the isoconfigurational run length to be 25 times shorter than that used for the propensity, which is evaluated at the end of the caging regime[19]. Fig. 4 shows that the propensity and number of new neighbors are heterogeneously distributed and correlated with each other — indicating that cage-escape dynamics of particles can be predicted to some extent by the rearrangements of Voronoi neighbors over a much shorter time.

Having established that acquiring new and losing old Voronoi neighbors is correlated with cage escape and hence particle diffusion, we ask what could be the elementary local motions by which new neighbors are acquired and old ones lost, and what local particle arrangements promote or preclude these motions. We consider the simplest class of local motions in which a single particle moves in its free volume, defined as the space within which its center can translate with other particles fixed.

A sufficient condition for a given particle to gain a new Voronoi neighbor is that at least one of its "exclusion spheres", i.e., the neighboring particles that define its free volume, is *not* currently one of its Voronoi neighbors (see Fig. 6a). In such a case, by moving within its free volume the given particle can touch the exclusion sphere, which certainly then becomes a new Voronoi neighbor. This criterion implies that the circumcenter of the Delaunay tetrahedron formed by the new Voronoi neighbor and three other neighboring exclusion spheres must be farther than σ from the original position of the given particle. Therefore, a cavity (into which an new sphere can be added) must exist. When a cavity is present, a nearby parti-

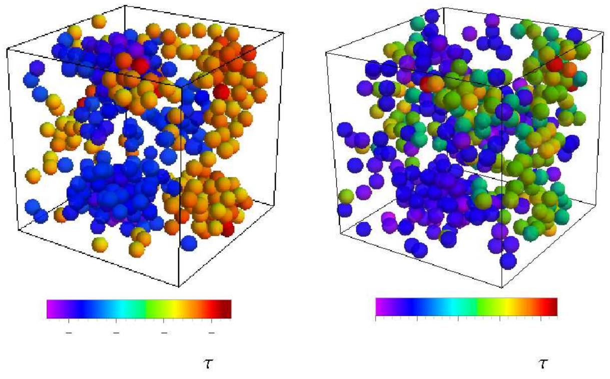

Fig. 4 Dynamic propensity (left) and number of new Voronoi neighbors (right) averaged at $\phi = 0.58$ over 400 isoconfigurational runs of length 125τ and 5τ respectively. 20% of particles with the largest and smallest values are shown for clarity. Propensity timescale 125τ corresponds to the end of the caging plateau in the log-log plot of MSD (see Fig. 1).

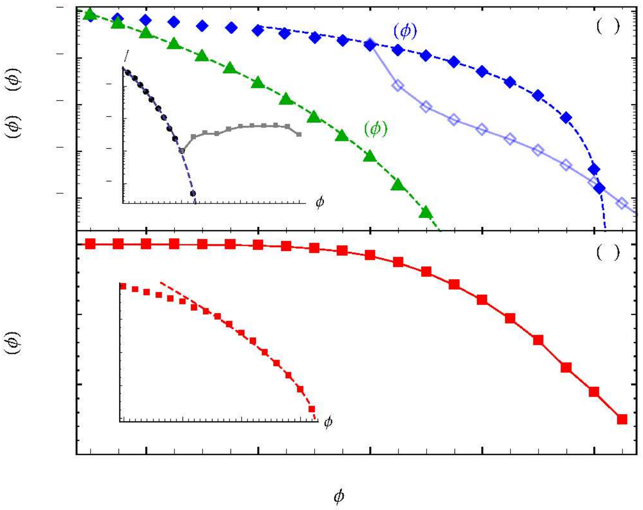

Fig. 5 (a) Diffusion coefficient $D(\phi)$ and uncaged particle fraction $h(\phi)$, versus volume fraction ϕ. Inset: average number of cavities per particle. (b) T1-active fraction $p_{\mathrm{T1}}(\phi)$. Inset: p_{T1} as ϕ approaches ϕ_0 (random close packing). All dashed lines are power law fits. The error bars are smaller the size of the symbols.

cle can hop into the cavity to acquire a new neighbor, leaving behind a cavity for another particle to hop into, and so forth. Stringlike motion observed in experiments[20] and simulations[19,21] seems to support this scenario. We call such a particle "uncaged", because it can move beyond its Voronoi cell without the aid of nearby particle motion.

To test this scenario, that uncaged particles contribute to neighbor rearrangements, we compute the fraction of uncaged particles $h(\phi)$ and number of cavities as a function of ϕ by extending the Sastry free volume construction[7] (see Fig. 5a). We find that cavities and hence uncaged particles become extremely rare, decreasing by four orders of magnitude as ϕ approaches 0.53 or so. By contrast, the diffusion coefficient $D(\phi)$ decreases much more gently with ϕ in this range. Thus uncaged particles cannot be primarily responsible for local neighbor rearrangements and structural relaxation in glassy hard-sphere fluids. (Note that we do observe a small concentration of cavities (vacancies) in the *crystal* phase, which lead to vacancy diffusion.)

If the sufficient but not necessary condition of uncaged particles is rarely met, how can particles in dense glassy change Voronoi neighbors when there is no cavity to hop into? By analogy to the T1 process of structural rearrangement in two dimensional foams[22] (see Fig. 6b), we identify another way particles can change neighbors. A particle p_1 with Voronoi neighbors p_2, p_3, p_4 can acquire a new Voronoi neighbor p_5, if p_1 is initially outside the circumsphere of the Delaunay tetrahedron formed by the four particles p_2–p_5, but is able to move inside the circumsphere to complete the T1 event. Note particle p_1 may have p_5 as a neighbor without being able to touch p_5. Through a reverse T1 event p_1 can lose p_5 as a neighbor.

The free volume of a given particle presents a set of cusps, each defined by three Voronoi neighbor particles. These cusps are the most favorable positions for a T1 event to occur. If a particle can either gain or lose a Voronoi neighbor while moving within its free volume, both it and the neighbor are marked as T1-active; otherwise, particles are T1-inactive.

The fraction of T1-active particles $p_{\mathrm{T1}}(\phi)$ as a function of ϕ is shown in Fig. 5b. In the fluid region $\phi < 0.5$, almost all particles are T1-active. In the metastable region $\phi > 0.5$, $p_{\mathrm{T1}}(\phi)$ decreases gently until ultimately vanishes near random close packing, as $(\phi_0 - \phi)^{\zeta}$, with $\phi_0 = 0.6448 \pm 0.0001$ and $\zeta = 0.65 \pm 0.02$. In contrast, the diffusion coefficient appears to vanish at the glass transition, at $\phi \approx 0.585$, which is associated with the growth of domains of particles that must rearrange cooperatively. Evidently, particle diffusion does not cease because T1-active particles become rare. Instead, we focus on T1-inactive particles, which by definition are those that cannot undergo T1 events by the motion of any single particle in the system.

For a T1-inactive particle to change Voronoi neighbors and contribute to structural relaxation, cooperative motion of at least two particles is required. Thus, formation of a network of T1-inactive particles could be related to the growth of cooperatively rearranging regions (CRRs). To this end, we study percolation of T1-inactive particles as volume fraction increases. We use particles that define the free volume of a given particle as its neighbors in the percolation problem. Spanning clusters (infinite in periodic boundary conditions) of T1-inactive particles are identified for many configurations over a range

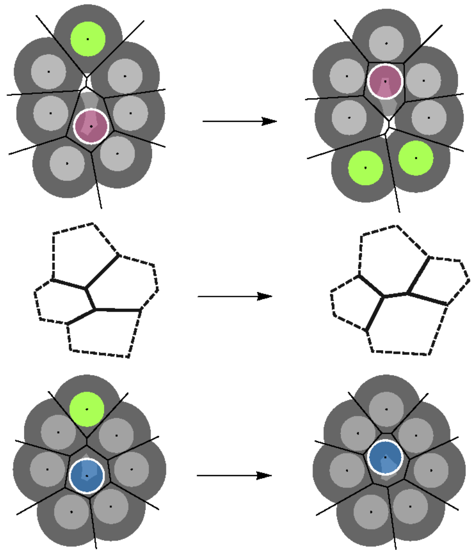

Fig. 6 2D schematics of neighbor rearrangements. (a) A hopping particle (purple) initially surrounded by its Voronoi neighbors (gray) can hop into the cavity (white region), collide with a new neighbor (green), and leave behind a cavity. (b) T1 event in a 2D foam corresponding to a flip of one soap film (solid line). (c) A T1-active particle (blue) gains a new neighbor (green) in a T1 event; no cavity is required.

of $\phi = 0.57$ to 0.61. The percolation threshold p_c and critical exponents are obtained from finite-size analysis.

Fig. 7 displays the percolation probability of T1-inactive clusters as a function of T1-inactive fraction $p_{\overline{\mathrm{T1}}}$. The inset shows the linear relation between T1-inactive fraction $p_{\overline{\mathrm{T1}}}$ and the particle volume fraction ϕ. Evidently, percolation of T1-inactive particles occurs around $p_{\overline{\mathrm{T1}}} = 0.232$, or equivalently $\phi = 0.59$. To obtain the critical threshold and exponents, we perform finite-size scaling by fitting the percolation probability as a function of T1-inactive fraction to a tanh function $\left(1+\tanh[(p_{\overline{\mathrm{T1}}} - p_{\mathrm{c}}^{\mathrm{eff}}(L))/\Delta(L)]\right)/2$ for different system sizes L, as shown in Fig. 7. In the limit of an infinite system, the percolation probability would be a step function and the percolation transition occurs at $p_{\mathrm{c}} = 0.232 \pm 0.002$, which corresponds to $\phi_{\mathrm{c}} \approx 0.586$ — essentially identical to the location of the "colloidal glass transition" often quoted as $\phi_{\mathrm{g}} \approx 0.585$[5,6]. The critical exponents in our model for the correlation length [$\xi \sim (\phi_{\mathrm{c}} - \phi)^{-\nu}$] and percolating cluster fraction [$m \sim (\phi - \phi_{\mathrm{c}})^{\beta}$] are $\nu = 0.91 \pm 0.01$ and $\beta = 0.50 \pm 0.02$, consistent with standard percolation results $\nu_0 \approx 0.88$ and $\beta_0 \approx 0.41$[23]. This suggests whatever spatial correlations in T1 activity are present are not strong enough to change the universality class.

In addition to our result that T1-inactivity percolates and the diffusion coefficient vanishes at the same volume fraction, we note that the scaling of the T1-inactive correlation length, combined with a power law fit for the vanishing diffusion coefficient [$D \sim (\phi_{\mathrm{c}} - \phi)^{-2.2\pm0.1}$], gives a dynamic scaling relation $1/D \sim \xi^z$ with $z \approx 2.4$. Similar values of $z \sim 2-5$ have been reported for power law relations between relaxation time and dynamic correlation length[24–26]. This is further evidence that T1-inactive clusters are dynamically relevant.

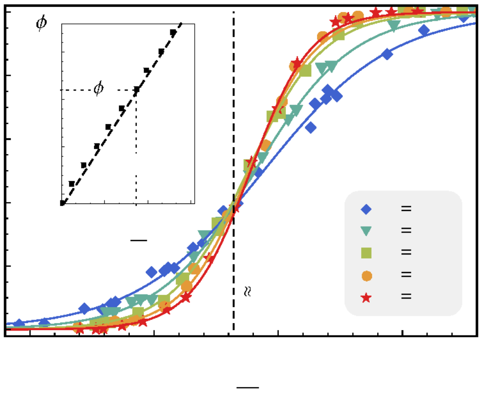

Fig. 7 Probability that a T1-inactive cluster spans the system as a function of T1-inactive fraction $p_{\overline{\mathrm{T1}}}$ for different system sizes; solid lines are fits to tanh function (see main text). Inset: volume fraction ϕ versus T1-inactive fraction $p_{\overline{\mathrm{T1}}}$.

In fact, a percolation approach to the glass transition has been suggested before. Cohen and Grest studied percolation of liquid-like particles with free volumes above some arbitrary criterion[27]. This approach seemed ad hoc, because no significant difference in free volume distribution distinguishes the liquid and glassy states. In contrast, the T1 activity of a particle by definition is determined from the configuration, the evolution of which is in turn influenced by the dynamics.

Recently, another connection between the glass transition and percolation has been reported[28]; namely, that the MCT glass transition ϕ_{c} coincides with the divergence of the cluster size of fast moving particles, and the VFT-fitted ϕ_0 (close to ϕ_{RCP}) coincides with the divergence of the cluster size of slow moving particles. Comparing this to the present work, we remark that fast and slow clusters are defined dynamically, based on observed particle mobility; both of them grow with increasing ϕ, consistent with increasing collective motion. In contrast, T1-activity is a purely geometrical property describing the "possibility" of changing Voronoi neighbors for a given configuration; the fraction of T1-inactive particles increases with increasing ϕ. The actual mobility of a particle in a given simulation is also influenced by the initial velocities, so there is no deterministic relation between T1-activity and mobility. That being said, an increasing number of T1-inactive particles, which cannot change their Voronoi neighbors by their individual motion, implies a growing degree of collective motion required for relaxation. The similar power law divergence of the dynamic correlation length and T1-inactive cluster length discussed above also suggests a connection between mobility and T1-inactive particles.

4 Summary

In this work, we have devised a crystal avoiding (CA) method, which can suppress crystallization in hard-sphere fluids while preserving the dynamics, to study glassy monodisperse hard-sphere fluids at $\phi > \phi_f$. The CA method allows us to explore glassy *monodisperse* hard-sphere fluids at $\phi > \phi_f$— for which equilibration has been a "subtle question"[29] — and offers new opportunities to examine the effect of polydispersity on dynamics. In searching for the relevant local rearrangements that permit particles to gain and lose Voronoi neighbors, we show that the number of uncaged particles vanishes too rapidly compared to the moderate slowing of diffusion, and so cannot be the primary means by which particles acquire new neighbors.

Instead, we propose that T1-active particles, identified based purely on geometry, are able to acquire and lose neighbors by single particle motion without cavities present, and are common enough to contribute to rearrangements, only becoming scarce near random close packing. Moreover, clusters of T1-inactive particles percolate at $\phi \approx 0.586$, remarkably close to the glass transition. These results suggest a close relation between T1-inactive clusters and slow dynamics in glassy hard-sphere fluids. Establishing the same link for polydisperse systems and exploring the possible connection of T1-(in)active correlation length to the dynamic or static correlation lengths will be the subject of future work.

References

1 P. Harrowell and A. Widmer-Cooper, *Phys. Rev. Lett.*, 2006, **96**, 185701.
2 A. Widmer-Cooper, P. Harrowell and H. Perry, *Nature Physics*, 2008, **4**, 711–715.
3 K. Chen, M. L. Manning, P. J. Yunker, W. G. Ellenbroek, Z. Zhang, A. J. Liu and A. G. Yodh, *Phys. Rev. Lett.*, 2011, **107**, 108301.
4 A. Widmer-Cooper and P. Harrowell, *J. Non-Cryst. Solids*, 2006, **352**, 5098–5102.
5 P. N. Pusey, E. Zaccarelli, C. Valeriani, E. Sanz, W. C. K. Poon and M. E. Cates, *Phil. Trans. R. Soc. A*, 2009, **367**, 4993–5011.
6 E. Zaccarelli, C. Valeriani, W. C. Poon, E. Sanz, M. E. Cates and P. N. Pusey, *Phys. Rev. Lett.*, 2009, **103**, 135704.
7 S. Sastry, D. S. Corti, P. G. Debenedetti and F. H. Stillinger, *Phys. Rev. E*, 1997, **56**, 5524.
8 J. Reinhardt, F. Weysser and M. Fuchs, *Phys. Rev. Lett.*, 2010, **105**, 199604.
9 W. van Megen and S. R. Williams, *Phys. Rev. Lett.*, 2010.
10 E. Zaccarelli, S. M. Liddle and W. C. K. Poon, *Soft Matter*, 2015, **11**, 324–330.
11 R. J. Speedy, *Journal of Physics: Condensed Matter*, 1999, **9**, 8591–8599.
12 C. Valeriani, E. Sanz, E. Zaccarelli, W. C. K. Poon, M. E. Cates and P. N. Pusey, *Journal of Physics: Condensed Matter*, 2011, **23**, 194117.
13 D. T. Limmer and D. Chandler, *J. Chem. Phys.*, 2011, **135**, 134503.
14 A. Reinhardt and J. P. K. Doye, *J. Chem. Phys.*, 2012, **136**, 054501.
15 P. Geiger and C. Dellago, *J. Chem. Phys.*, 2013, **139**, 164105.
16 W. Lechner and C. Dellago, *J. Chem. Phys.*, 2008, **129**, 114707.
17 M. Skoge, A. Donev, F. H. Stillinger and S. Torquato, *Phys. Rev. E*, 2006, **74**, 041127.
18 P.-R. ten Wolde, M. J. Ruiz-Montero and D. Frenkel, *Faraday Disc.*, 1996, **104**, 93.
19 A. Widmer-Cooper, P. Harrowell and H. Fynewever, *Phys. Rev. Lett.*, 2004, **93**, 135701.
20 E. R. Weeks, J. C. Crocker, A. C. Levitt, A. Schofield and D. A. Weitz, *Science*, 2000, **287**, 627–631.
21 W. Kob, C. Donati, S. C. Glotzer, P. H. Poole and S. J. Plimpton, *Phys. Rev. E*, 1999, **60**, 3107.
22 M. Durand and H. A. Stone, *Phys. Rev. Lett.*, 2006, **97**, 226101.
23 A. Aharony and D. Stauffer, *Introduction To Percolation Theory*, Taylor & Francis, 2003.
24 N. Lačević, F. W. Starr, T. B. Schrøder and S. C. Glotzer, *J. Chem. Phys.*, 2003, **119**, 7372.
25 S. Whitelam, L. Berthier and J. Garrahan, *Phys. Rev. Lett.*, 2004, **92**, 185705.
26 E. Flenner, M. Zhang and G. Szamel, *Phys. Rev. E*, 2011.
27 M. H. Cohen and G. S. Grest, *Ann. N. Y. Acad. Sci.*, 1981, **371**, 199–209.
28 Z. Zheng, R. Ni, F. Wang, M. Dijkstra, Y. Wang and Y. Han, *Nature Communications*, 2014, **5**, 3829.
29 M. D. Rintoul and S. Torquato, *Phys. Rev. Lett.*, 1996, **77**, 4198–4201.